

# MALDI PSD of low molecular weight ethoxylated polymers

Scott D. Hanton<sup>a,\*</sup>, David M. Pares<sup>a</sup>, Kevin G. Owens<sup>b</sup>

<sup>a</sup> Air Products and Chemicals Inc., 7201 Hamilton Blvd., Allentown, PA 18195, USA

<sup>b</sup> Department of Chemistry, Drexel University, Philadelphia, PA 19104, USA

Received 10 March 2003; accepted 21 September 2004

## Abstract

Matrix-assisted laser desorption/ionization (MALDI) mass spectrometry has become an important technique to characterize the chemical structure of industrial polymer materials. MALDI methods have been developed to address a broad variety of different polymer materials, containing different chemistries. One of the key aspects of the typical MALDI experiment is the generation of intact molecular ions. The development of MALDI post-source decay (PSD) techniques has opened a new method to obtain chemical structure information from MALDI experiments. PSD provides an accessible MALDI MS/MS experiment that can be done on most commercial time-of-flight (TOF) reflectron instruments. MALDI PSD techniques have been successfully applied to a variety of synthetic polymers. This work explores the applicability of MALDI PSD methods to relatively low molecular weight ethoxylated surfactants. In these experiments, we show the PSD fragmentation mass spectra of some ethoxylated surfactants, explore the mechanisms for the fragmentations, investigate the effect of different alkali cations, and compare the fragments from isobaric surfactant molecules.

© 2004 Elsevier B.V. All rights reserved.

**Keywords:** Matrix-assisted laser desorption/ionization; MALDI; Time-of-flight mass spectrometry; TOFMS; Post-source decay; PSD; Fragmentation; Ethoxylated surfactants; Surfynol® surfactants

## 1. Introduction

Matrix-assisted laser desorption/ionization (MALDI) mass spectrometry [1–4] has become an important technique to characterize the chemical structure of industrial polymer materials [5–7]. MALDI can generate important data on the telomer repeat units, end groups, and average molecular weights of these materials. MALDI methods have been developed to address a broad variety of different polymer materials, containing different chemistries. One of the key aspects of the typical MALDI experiment is the generation of intact molecular ions. MALDI mass spectra generally show little fragmentation. The production of intact ions is vital for the quantitation of average molecular weights, but limits the amount of chemical structural information that can be obtained from the data.

The development of MALDI post-source decay (PSD) techniques has opened a new method to obtain chemical structure information from MALDI experiments [8,9]. PSD provides an accessible MALDI MS/MS experiment that can be done on most simple, commercial time-of-flight (TOF) reflectron instruments [10] and does not require the more complex and expensive quadrupole-orthogonal TOF, hybrid magnetic sector or Fourier transform mass spectrometer (FTMS) instruments used to conduct the traditional collision-induced dissociation (CID) MS/MS experiments. It needs to be noted here that the traditional CID MS/MS experiments generally produce superior data to PSD data.

In PSD, the desired ion is selected in the linear portion of the TOF flight tube using an electrostatic gate near the source. The mass resolution at this point in the experiment is not very high, so a relatively broad range of masses is selected, compared to a traditional MS/MS experiment on a sector instrument. The ions arriving at the gate at the desired time will pass into the TOFMS. Fragmentation in PSD is accomplished by

\* Corresponding author. Tel.: +1 610 481 8036; fax: +1 610 481 6578.  
E-mail address: [hantonsd@airproducts.com](mailto:hantonsd@airproducts.com) (S.D. Hanton).

significantly increasing the desorption laser fluence, which increases the number of gas phase species escaping the surface of the sample and expanding in the desorption plume. The greater plume density increases the number of collisions experienced by the selected ion(s). In a typical MALDI experiment, the laser fluence is minimized to generate improved mass accuracy and mass resolution. In a PSD experiment, however, the laser fluence is increased until significant fragmentation is observed. The energy for the metastable decay is delivered from the gas phase collisions, not from directly absorbing the laser light. In many commercial TOF instruments, PSD spectra are acquired by scanning the reflectron voltage and collecting the fragment spectrum in several segments.

MALDI PSD was initially reported for experiments on proteins and peptides and there have been numerous reports of biomolecule PSD fragmentation spectra [8]. It is a valuable method employed to sequence unknown peptides. The PSD technique has also been successfully applied to a variety of synthetic polymers [11–16]. These experiments have demonstrated the capability of PSD experiments to create useful MS/MS data on polymer analytes, often shedding light on the chemical structure of these materials.

This work explores the applicability of MALDI PSD methods to relatively low molecular weight ethoxylated surfactants. Many of these materials are known to generate intense MALDI mass spectra [17]. We wish to see if they will also generate useful PSD fragmentation spectra. If so, we will be able to use MALDI to probe further into the chemical structures of these materials. We will also investigate the effect of different alkali cations, compare isobaric surfactant molecules, and compare gemini surfactants to those containing single ethoxylate chains.

While a variety of ethoxylated surfactants will be explored in these experiments, the bulk of the experiments are focused on Surfynol<sup>®</sup> 4XX (S4XX, XX = 40, 65, and 85), a commercially available series of telomeric ethoxylated surfactants. The increasing XX values indicate increasing amounts of ethoxylation on a backbone of 2,4,7,9-tetramethyl-5-decyne-4,7-diol (Surfynol<sup>®</sup> 104), as shown in Fig. 1.

The performance of these materials as surfactants depends on the degree of ethoxylation. Surfynol<sup>®</sup> surfactants offer several advantages: rapid migration, low dynamic surface tension, defoaming, FDA compliance, and stability in high electrolyte brine systems.

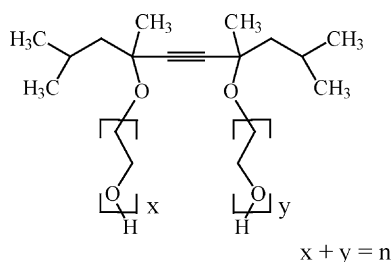


Fig. 1. The chemical structure of the S4XX surfactants.

One of the motivators of this work is to evaluate the capability of MALDI PSD to elucidate the relative chain length isomers of the S4XX telomers. The two EO chains, X and Y, can vary in size yet have the same mass. Previous studies showed that chain length isomers could be differentiated by gas chromatography (GC), but not by single MS experiments [17]. Unfortunately, many of these materials have too high a degree of polymerization to be analyzed by GC. If PSD can measure the individual chain length isomers, we can extend our study to higher mass telomers.

## 2. Experimental

### 2.1. Chemicals

The S4XX samples were obtained from Air Products and Chemicals, Inc. (Allentown, PA). The polyethylene glycol (PEG) 1000 sample was obtained from Sigma–Aldrich Fine Chemicals, Inc. (Milwaukee, WI). The ethoxylated octadecanol was obtained from BASF. The samples were prepared for MALDI using the matrices 2,5-dihydroxybenzoic acid (DHB) and alpha-cyano-4-hydroxycinnamic acid (CHCA), which were both obtained from Sigma–Aldrich. Samples doped with a specific alkali salt used the Li, Na, or K hydroxides obtained from Aldrich. All chemicals were used as received. The PSD spectra were calibrated using ACTH clip 18-39 obtained from Sigma–Aldrich.

### 2.2. Sample preparation

Analytes were prepared as 5 mg/ml solutions in methanol or tetrahydrofuran (THF). All of the analytes in this study were readily soluble in either solvent. The analyte solutions were mixed 1:7 by volume with 0.25 M matrix solutions in the same solvent. If a sample was doped with a particular alkali cation, an equal amount to the analyte solution of an 0.025 M MOH (where M = Li, Na, or K) solution was added. In most cases, Na was not added to these samples. If the samples were prepared in soft glass vials, sufficient Na was present in the samples. If Na needed to be excluded from the sample preparation, then the samples were prepared in plastic vials. All samples were deposited by the dry drop method using approximately 0.5–1.0  $\mu\text{l}$  of the mixed solution. Samples were allowed to dry under ambient conditions. One 0.5  $\mu\text{l}$  deposition provided sufficient sample for at least two PSD experiments.

### 2.3. Mass spectrometry

All of the MALDI experiments were conducted on a Bruker Biflex III (Billerica, MA) TOF mass spectrometer. These experiments were all conducted in reflectron mode using delayed extraction. The Biflex was equipped with a nitrogen laser operated at 337 nm. For normal MALDI, the laser fluence was minimized to just above threshold for ions. In

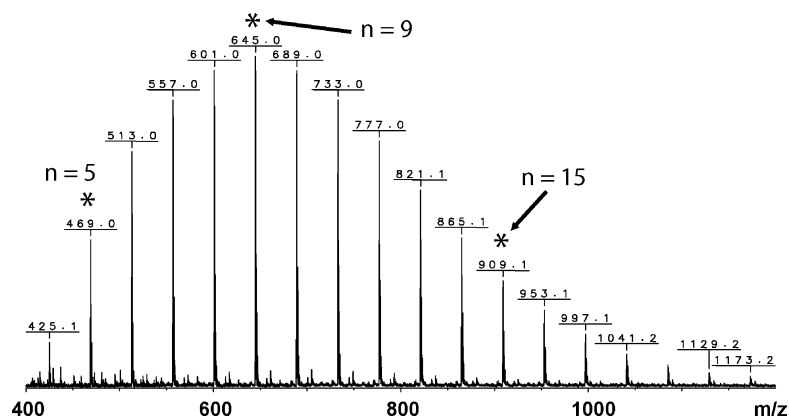


Fig. 2. MALDI mass spectrum of S465 + Na<sup>+</sup> showing three telomers of interest, 469, 645, and 909 D.

PSD mode, the laser fluence was increased producing significant fragmentation. The source conditions of the mass spectrometer were optimized for mass resolution around 1000 D. Spectra were collected by moving the laser around the surface of the sample and averaging 100 shots/spectrum. The data were analyzed using Bruker Xtof software set for average segments mode. The mode used to stitch the segments together does impact the relative peak heights of the fragment ions.

To obtain the PSD spectra, the ion gate was optimized for the target analyte ion. Typically, the gate was set for  $\pm 20$  D. With a 44 D spacing between the telomers, this was sufficiently narrow to exclude signal from adjacent telomers, but sufficiently wide to maintain high ion transmission. The PSD spectra were obtained by collecting 14 segment mass spectra, each with a different reflectron voltage. It is critical to ensure that the reflectron is properly aligned to collect meaningful PSD spectra [18]. The segment spectra are each calibrated using the well-established PSD spectrum of ACTH clip. We calibrated ACTH in both DHB and CHCA, but observed little difference in the results. The relatively poor mass resolution and mass accuracy of the PSD data obscured any meaningful difference between the two matrices.

### 3. Results and discussion

Fig. 2 shows the MALDI mass spectrum of a sample of S465 surfactant with sodium cationization. We readily measure the distribution of ethoxylated telomers and can verify the repeat units, end group mass and measure the average molecular weights. The PSD gate on the Biflex can easily isolate a single telomer from this distribution. In more complex samples, more than one species may be passed through the gate. The minimum gate width for these experiments was about  $\pm 10$  D. In Fig. 2, three telomer ions are highlighted,  $n = 5$  at 469 D,  $n = 9$  at 645 D, and  $n = 15$  at 909 D. Individual PSD spectra will be discussed for these three telomers.

Fig. 3 shows the PSD mass spectrum generated from the 469 D ion. Even after increasing the laser fluence to initiate metastable decay, the target ion is still much more intense than the fragment ions, and is far off scale in the figure. This is a typical PSD spectrum from a relatively low degree of polymerization telomer. The key ion in the PSD spectrum is the 259 D fragment. This represents the loss of 210 D from the precursor ion and is followed by subsequent fragments spaced by 44 D. We see this as the major fragment series for all of the S4XX analytes studied. In Fig. 3, we also see a significant Na<sup>+</sup>

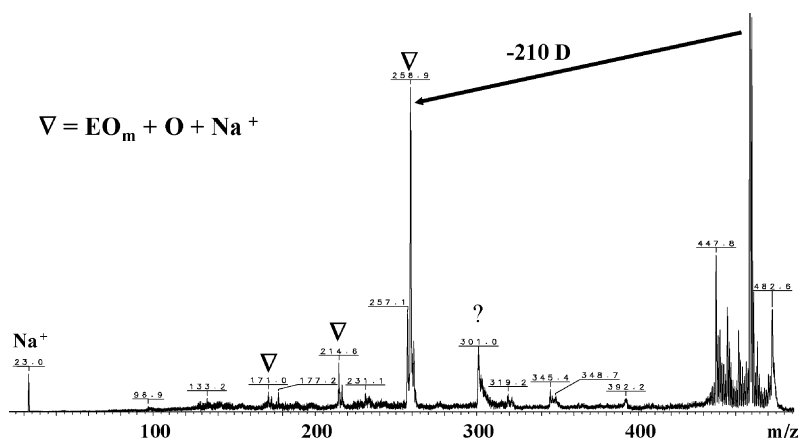


Fig. 3. MALDI PSD mass spectrum of the  $n = 5$  (469 D) ion showing the primary fragmentation pathway of the loss of 210 D.

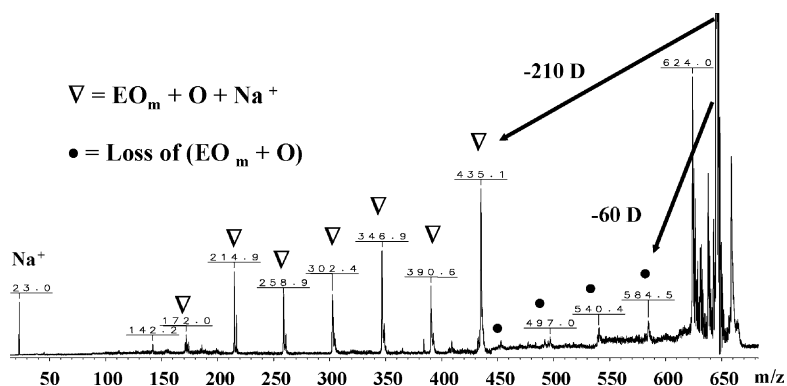


Fig. 4. MALDI PSD mass spectrum of the  $n=9$  (645 D) ion showing two different fragmentation pathways. The primary pathway is the loss of 210 D, and the minor pathway is the loss of 60 D.

ion at 23 D. This indicates that separation of the metal cation from the neutral surfactant is an important PSD pathway. For these analytes, the  $\text{Na}^+$  ion intensity is relatively low compared to that of the other fragments, indicating that the  $\text{Na}^+$  is strongly bound to the surfactant [19]. That the breaking of covalent bonds is preferred to loss of the attached cation is consistent with a charge remote fragmentation mechanism [20,21]. In addition to these ions, we also see some less well-resolved ions between 300 and 400 D that are not assigned. We see some 44 D spacing among these ions, which indicates that the EO chains are involved in these fragmentations.

Fig. 4 shows the PSD spectrum of the  $n=9$  telomer at 645 D. Again we see the major fragmentation pathway is the loss of 210 D leading to a series of peaks spaced by 44 D. We see some loss of the Na cation, and we see a new series starting with a 60 D loss from the precursor and having several 44 D steps. The main fragmentation series has ions that are spaced by 2 D. This is typical of PEG collision-induced dissociation (CID) as described in the fundamental work by Selby et al. [22]. These EO chains create PSD fragments similar to the CID fragmentation of PEG telomers observed in [22].

Fig. 5 shows the PSD spectrum of the  $n=15$  telomer at 909 D. This PSD spectrum contains all of the features observed for the  $n=9$  telomer in Fig. 4, plus a new significant fragment at  $-161$  D from the precursor that shows no 44 D

spaced peaks. Since the other two main fragment paths show peaks spaced by 44 D, they must involve the EO chains. This new fragment must follow an unrelated mechanism.

The main PSD fragment observed for the S4XX telomers is the loss of 210 D from the precursor, followed by a series of ions spaced by 44 D. The hydrophobe in the material, which has a mass of 226 D. To lose 210 D, the fragmentation must involve the hydrophobe. Also, all of the EO units in both chains are part of the fragment ion. In Fig. 4, the most intense fragment must have all 9 EO units from the precursor. We can see fragments in the series, containing from 3 to 9 EO units. Fragments smaller than 3 EO units will not have sufficient cationization stability to retain the  $\text{Na}^+$  charge [17,19], remain ions, and be observed in the experiment.

For all of the EO units to remain in the fragment, at least two covalent bonds must break to separate both EO chains from the hydrophobe. Simpler mechanisms, based on the work of Selby et al. [22] were examined, but did not fit some features of the data. These mechanisms were developed from molecules with a single ethoxy chain, which produce several different fragment series, some of which are missing in our spectra. Also, the Surfynol<sup>®</sup> surfactant analytes in this work are molecules with two ethoxy chains with multiple chain length isomers for each molecular weight (as described

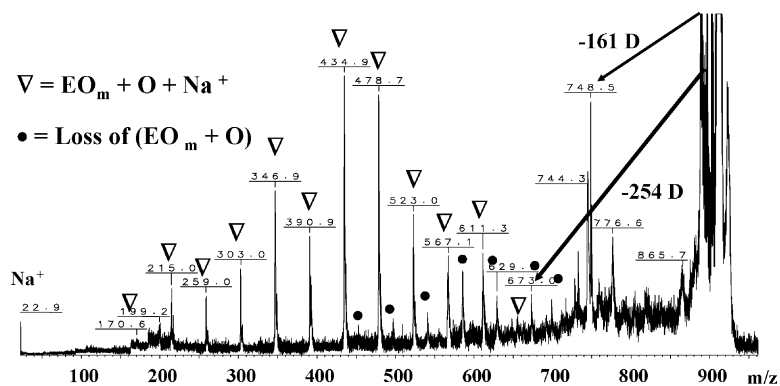


Fig. 5. MALDI PSD mass spectrum of the  $n=15$  (909 D) ion showing the three different fragmentation pathways.

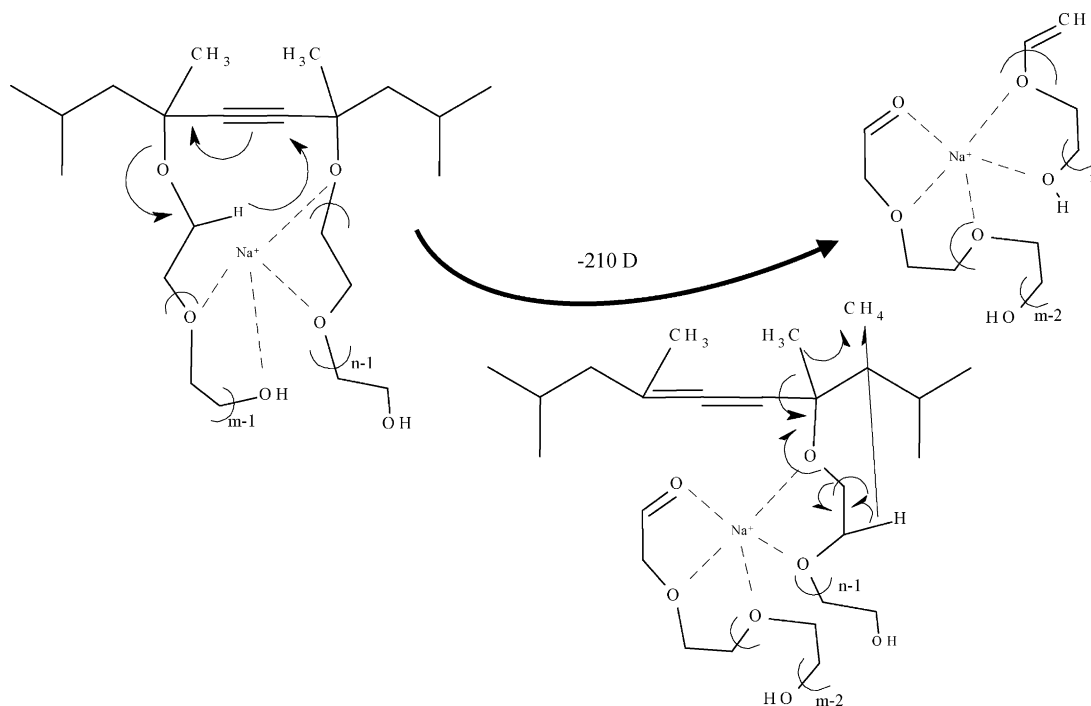


Fig. 6. Schematic showing the proposed fragmentation mechanism to generate the loss to 210 series observed in the MALDI PSD mass spectra of the S4XX telomers.

above). If the simpler mechanisms were applicable, the spectra would show chain length isomer distributions [17]. Instead, we observe no chain length isomer dependence in the PSD data. The suggested mechanism is consistent with all of this data, but is not proved by it. If we extend the mechanisms published by Selby et al. [22] and invoke the concepts of charge remote fragmentation [20] we can generate the mechanism shown in Fig. 6.

The mechanism we suggest for the series beginning with  $-210\text{D}$  loss begins with a hydrogen transfer from an EO unit to the alkyne bond, electron density transfer converting the alkyne bond into an allene, and the breaking of the bond between the tertiary ether and the hydrophobe. The initial hydrogen transfer is a McLafferty type rearrangement [23] and the conversion of alkyne to allene functions is known from solution phase organic chemistry [24,25]. On the opposite side of the molecule, we propose a hydrogen transfer from the EO unit adjacent to the tertiary ether to either the methyl or butyl group on the S104 backbone, electron density transfer from the EO unit to the tertiary ether oxygen bond to the backbone, and electron density transfer from the methyl or butyl group to the tertiary ether oxygen bond to the backbone creating a ketone moiety, a neutral alkane molecule and severing the bond between the oxygen atom and the rest of the EO chain. At this time, we have no data to determine if either methane or butane is mainly produced during the fragmentation. Perhaps in the future, a reionization experiment could be done to investigate the neutral parts of the mechanism. This mechanism is consistent with the observed fragment ion peaks in these molecules. The remaining fragment ion observed in

the mass spectrometer begins to look like a crown ether in its interactions with the cation. The primary difference being that the two EO chains are only connected through the cation interaction.

The key to this series of fragment ions is the interactions between the EO chains and the cation. Previous work has shown that the cation can bring the two chains of the S4XX gemini surfactant together to maximize the interaction [19]. With this fragmentation mechanism, these interactions are shown to be stronger than covalent bonds in the molecule. It is also interesting to note that the distribution of fragment ions in this series peaks around  $n=9$  at 435 D. If a telomer has fewer than or equal to 9 EO units, then the most intense fragment is the peak containing all of the EO units, as shown in Figs. 3 and 4. For telomers with more than 9 EO units, the most intense fragment peak is around the 435 D ion, as shown in Fig. 5. This distribution is providing information about the relative stability of the Na cation interaction with the EO chains. While we generate no structural information about these fragments from these experiments, the peak at  $n=9$  generally agrees with previous experiments optimizing the number of oxygen atoms surrounding the Na cation in MALDI drift tube experiments reported by Bowers and co-workers [26].

The other fragmentation series observed in the higher mass telomers is shown in Fig. 4 for the  $n=9$  telomer. The fragment series begins  $-60\text{D}$  from the precursor ion and extends with 44 D spacing. By mass, this loss corresponds to  $\text{EO}_m + \text{O}$ . One possible assignment could be the loss of  $\text{HO}-(\text{EO}_{m-1})-\text{CH}_2\text{CHO}$ . It probably represents the loss of EO units near

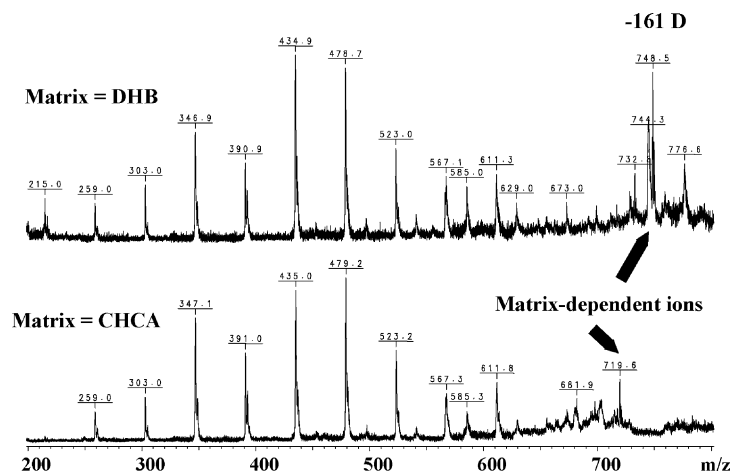


Fig. 7. Comparison of MALDI PSD mass spectra for the  $n = 15$  (909 D) ions prepared using DHB (top) and CHCA (bottom). The  $-161$  D fragment ion observed in DHB is not observed when prepared in CHCA.

or at the ends of the EO chains. In these cases, the charge remains with the bulk of the EO units and the hydrophobe backbone. These fragments are interpreted to also be charge remote fragmentation, which involves an H transfer to the new end unit of the chain. This would indicate that these EO units are sufficiently far from the Na cation to not be involved in its stability. We only observe this series for the longer chain telomers because the molecule requires an excess of EO units to exhibit this fragmentation path.

Another fragment ion starts to appear for the  $n = 11$  and higher telomers. We see a fragment at  $-161$  D from the precursor ion that is not part of a series of related fragment ions. We also observe this particular fragment from a number of other ethoxylated surfactants (see discussion below). Considering the fragmentation mechanisms operating for the other fragment paths, this ion appears incongruous. To explore this fragmentation further, we prepared the S465 sample in THF with the CHCA matrix. Fig. 7 shows a comparison of the PSD spectra obtained from the  $n = 15$  telomer in DHB (top) and CHCA (bottom). Both spectra clearly show the main fragmentation series. Up to about 650 D, the two spectra are

essentially the same. Between 650 and 800 D, however, we see significant differences between the two PSD spectra. The ion of interest, the  $-161$  D fragment, is not observed in the CHCA matrix. Experiments with matrix blanks, even with additional sodium added, do not produce these  $-161$  PSD fragments in experiments on our Bruker Biflex [27]. It appears that both the polymer and the matrix must be present in the sample for us to observe these species. We contend that the  $-161$  D ion is a result of some interaction between the S4XX telomer and the matrix. We also see some lower intensity ion peaks in the PSD spectrum from CHCA, such as the 719 D ion that appears to be the result of some matrix–analyte interaction. The nature of the matrix–analyte interaction leading to this fragmentation path will be the focus of new investigations and will be reported separately.

In each of the fragmentation paths discussed, the two EO chains of the S4XX telomers work in concert to generate the observed fragment ions. While we often see fragment ions in the ion series that account for almost all of the EO units in the chains, we cannot get information from these experiments about the chain length isomers. The interaction between the

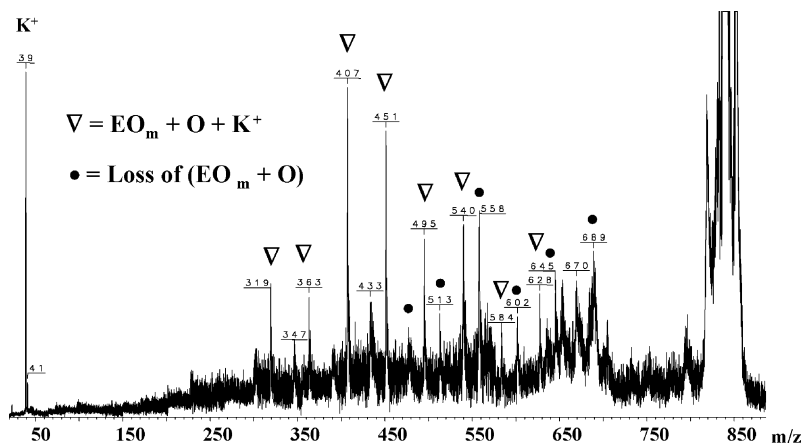


Fig. 8. MALDI PSD mass spectrum for the  $n = 13$  (837 D) ion.

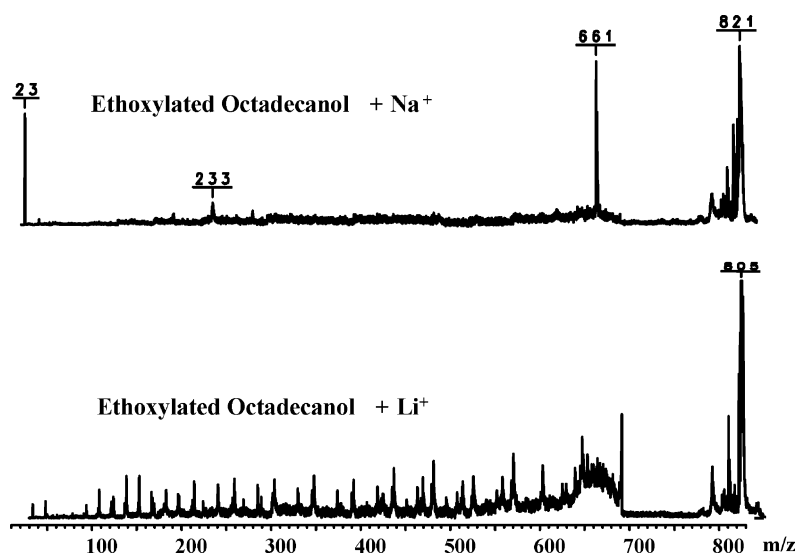


Fig. 9. Comparison of MALDI PSD mass spectra for the  $n = 12$  telomer of an ethoxylated octadecanol surfactant cationized with Na (top) and with Li (bottom). The Li-cationized ion produces a much richer fragmentation spectrum.

EO units and the Na cation are too strong to separate the two chains and observe them independently. Unfortunately, PSD will not provide the data we were originally looking for to elucidate the chain length isomers for non-volatile telomers.

If we change the cation from Na to Li in these experiments, we observe nearly the same PSD spectra. The  $-210$  D fragment series still dominates the PSD spectra. The peak of the distribution of 44 D spaced peaks is still between 8 and 9 EO units. The  $-161$  D fragment is still observed, but doesn't appear until higher telomer number and is greatly broadened in the PSD spectrum compared to the other fragments. It is surprising that the distribution of EO units from the  $-210$  D fragment series peaks at the same number of EO units for both Na and Li-cationized species. Previous work by the Bowers group indicates that the Li cation typically has fewer oxygen atoms around it than a Na cation in experiments on PEG [28]. We expected the Li-cationized species to peak at a smaller number of EO units than the Na-cationized species.

If we change the cation from Na to K in these experiments, we observe much weaker PSD fragment ion intensity. Fig. 8 shows the PSD mass spectrum obtained from the  $n = 13$  telomer of S465 cationized with K. We observe a very intense  $K^+$  ion at 39 D indicating that the loss of the cation is the most prominent metastable fragmentation path for these species. The K cation must not interact with the two EO chains nearly as well as Li and Na cations [28]. We still observe the other two fragmentation mechanisms, but the ion signal is quite weak. Interestingly, the center of the  $-210$  D fragment series is again between 8 and 9 EO units, just like the Na- and Li-cationized species.

While these data show that there is only a limited cation effect in the metastable decay of the S4XX telomers, we have observed much more pronounced cation effects in single chain ethoxylated surfactants. Fig. 9 shows two PSD spectra

obtained from the  $n = 12$  telomer of an ethoxylated octadecanol surfactant. At the top of the figure, is the PSD spectrum from the Na-cationized telomer and at the bottom of the figure is the PSD mass spectrum of the Li-cationized telomer. The Na-cationized species shows only two significant fragments, the Na cation and a  $-160$  D ion. As with the  $-161$  D ion observed for the S4XX telomers (discussed above), this ion is matrix dependent and must be some type of matrix adduct. In contrast, the Li-cationized telomer produces a rich mass spectrum with many interesting fragment ions. Experiments on PEG telomers produce the same results. The rich PSD spectrum obtained for Li-cationized PEG is essentially the same as the CID results previously discussed by Selby et al. [22]. The Li-cationized PSD spectra of both the PEG and the ethoxylated octadecanol surfactant can be understood by following the descriptions of the CID experiments in [22].

For these surfactants, the metastable decay results appear to significantly depend on the difference between a single EO chain surfactant and a gemini surfactant. The S4XX gemini surfactants interact sufficiently with the Na cation to produce intense and information-rich PSD spectra. The single chain ethoxylated surfactants investigated do not interact sufficiently with a Na cation, but do interact strongly with a Li cation.

This difference in PSD fragmentation can also be used to investigate isobaric analytes. The S4XX and ethoxylated octadecanol surfactants have the same nominal mass when comparing telomers differing by one EO unit. The octadecanol backbone has mass 44 D greater than the S104 backbone. We have utilized the difference in PSD response for Na-cationized analytes to clearly distinguish which surfactant is present in unknown samples. The PSD experiment is relatively easy to conduct and, in this case, provides unambiguous identification of the surfactants.

## Acknowledgements

We thank Air Products and Chemicals Inc., for their support of this research, Mr. Armin Holle from Bruker Daltonics for help optimizing the performance of our Biflex TOF instrument, Mr. Andrew Hoteling from Kodak for helpful discussions regarding PSD calibration and the matrix dependence of some PSD fragment ions, Prof. Michael Gross from Washington University for helpful discussions about charge remote fragmentation and the possible mechanisms involved in the PSD fragmentation of the S4XX surfactants, Drs. Tony Jackson and Jim Scrivens from ICI for detailed discussion of possible fragmentation mechanisms and Drs. John Sadowski and Kevin Lassila for critical review of the manuscript.

## References

- [1] K. Tanaka, H. Waki, Y. Ido, S. Akita, Y. Yoshido, T. Yoshido, Protein and polymer analyses up to  $m/z$  100,000 by laser ionization time-of-flight mass spectrometry, *Rapid Commun. Mass Spectrom.* 2 (1988) 151.
- [2] M. Karas, F. Hillenkamp, Laser desorption ionization of proteins with molecular masses exceeding 10,000 Da, *Anal. Chem.* 60 (1988) 2299.
- [3] U. Bahr, A. Deppe, M. Karas, F. Hillenkamp, U. Giessman, Mass spectrometry of synthetic polymers by UV-matrix-assisted laser desorption/ionization, *Anal. Chem.* 64 (1992) 2866.
- [4] P. Danis, D. Karr, F. Mayer, A. Holle, C. Watson, The analysis of water-soluble polymers by matrix-assisted laser desorption time-of-flight mass spectrometry, *Org. Mass Spectrom.* 27 (1992) 843.
- [5] S.D. Hanton, Mass spectrometry of polymers and polymer surfaces, *Chem. Rev.* 101 (2) (2001) 527.
- [6] M.W.F. Nielen, MALDI time-of-flight mass spectrometry of synthetic polymers, *Mass Spectrom. Rev.* 18 (1999) 309.
- [7] R. Roli, in: G. Montaudo, R.P. Lattimer (Eds.), *Mass Spectrometry of Polymers*, CRC Press, Boca Raton, FL, 2002.
- [8] R. Kaufman, D. Kirsch, B. Spengler, *Int. J. Mass Spectrom. Ion Proc.* 165/166 (1997) 405.
- [9] B. Spengler, D. Kirsch, R. Kaufmann, Fundamental aspects of post-source decay in matrix-assisted laser desorption mass spectrometry, *J. Phys. Chem.* 96 (1992) 9678.
- [10] J. Franzen, R. Frey, A. Holle, K.H. Kraeuter, Recent progress in matrix-assisted laser desorption ionization postsource decay, *Int. J. Mass Spectrom.* 206 (2001) 275.
- [11] U. Puapaboon, R.T. Taylor, J. Jai-nhuknan, Structural confirmation of polyurethane dendritic wedges and dendrimers using post source decay matrix-assisted laser desorption/ionization time-of-flight mass spectrometry, *Rapid Commun. Mass Spectrom.* 13 (1999) 516.
- [12] I. Fournier, A. Marie, D. Lesage, G. Bolbach, F. Fournier, J.C. Tabet, Post-source decay time-of-flight study of fragmentation mechanisms of protonated synthetic polymer under matrix-assisted laser desorption/ionization conditions, *Rapid Commun. Mass Spectrom.* 16 (2002) 696.
- [13] L. Przybilla, V. Francke, H.J. Raeder, K. Muellen, Block length determination of a poly(ethylene oxide)-*b*-poly(*p*-phenylene ethynylene) diblock copolymer by means of MALDI-TOF mass spectrometry combined with fragment-ion analysis, *Macromolecules* 34 (2001) 4401.
- [14] L. Przybilla, H.J. Raeder, K. Muellen, Post-source decay fragment ion analysis of polycarbonates by matrix-assisted laser desorption/ionization time-of-flight mass spectrometry, *Eur. Mass Spectrom.* 5 (1999) 133.
- [15] J.H. Scrivens, A.T. Jackson, H.T. Yates, M.R. Green, G. Critchley, J. Brown, R.H. Bateman, M.T. Bowers, J. Gidden, The Effect of the variation of cation in the matrix-assisted laser desorption/ionisation-collision-induced dissociation (MALDI-CID) spectra of oligomeric systems, *Int. J. Mass Spectrom. Ion Proc.* 165/166 (1997) 363.
- [16] R.J. Goldschmidt, S.J. Wetzel, W.R. Blair, C.M. Guttman, Post-source decay in the analysis of polystyrene by matrix-assisted laser desorption/ionization time-of-flight mass spectrometry, *J. Am. Soc. Mass Spectrom.* 11 (1998) 1095.
- [17] D.M. Parees, S.D. Hanton, P.A. Cornelio Clark, D.A. Willcox, Comparison of mass spectrometric techniques for generating molecular weight information on a class of ethoxylated oligomers, *J. Am. Soc. Mass Spectrom.* 9 (1998) 282.
- [18] The alignment of the Biflex reflectron requires an off center optimization to account for the difference in flight path for fragments and intact molecules to the detector. We wish to gratefully thank Armin Holle from Bruker Daltonics for spending extra time with us explaining this important point and properly aligning our instrument.
- [19] H. Cheng, P.A. Cornelio Clark, S.D. Hanton, P. Kung, Cationization effect on the molecular weight distribution of an ethoxylated polymer: a combined theoretical and time-of-flight secondary ion mass spectroscopic study, *J. Phys. Chem. A.* 104 (2000) 2641.
- [20] M.L. Gross, Charge-remote fragmentation: an account of research on mechanisms and applications, *Int. J. Mass Spectrom.* 200 (2000) 611.
- [21] C. Cheng, M.L. Gross, Applications and mechanisms of charge-remote fragmentation, *Mass Spectrom. Rev.* 19 (2000) 398.
- [22] T.L. Selby, C. Wesdemiotis, R.P. Lattimer, Dissociation characteristics of  $[M+X]^+$  ions ( $X=H, Li, Na, K$ ) from linear and cyclic polyglycols, *J. Am. Soc. Mass Spectrom.* 5 (1994) 1081.
- [23] F.W. McLafferty, F. Turecek, *Interpretation of Mass Spectra*, fourth ed., University Science Books, Mill Valley, CA, 1993.
- [24] J. Wotiz, in: H.G. Viehe (Ed.), *Chemistry of Acetylenes*, Marcel-Dekker, NY, 1969, p. 371.
- [25] J. March, *Advanced Organic Chemistry*, third ed., Wiley-Interscience, NY, 1985, pp. 525.
- [26] G. von Helden, T. Wyttenbach, M.T. Bowers, Inclusion of a MALDI ion source in the ion chromatography technique: conformational information on polymer and bimolecular ions, *Int. J. Mass Spectrom. Ion Proc.* 146/147 (1995) 349.
- [27] Unpublished results from Andrew Hoteling of Kodak indicate that  $-161$  D ions have also been observed in his Micromass Tofspec instrument. In fact, he also observes these fragments in matrix blank experiments. We have not been able to reproduce these blank results on our Bruker Biflex instrument. Perhaps these results are instrument specific. We would welcome other instrument users to reproduce these experiments and provide data for these conclusions.
- [28] T. Wyttenbach, G. von Helden, M.T. Bowers, Conformations of alkali cationized polyethers in the gas phase: polyethylene glycol and bis(benzo-15-crown-5)-15-ylmethyl] pimelate, *Int. J. Mass Spectrom. Ion Proc.* 165/166 (1997) 377.